European Journal of Cardio-Thoracic Surgery 49 (2016) 93–100
doi:10.1093/ejcts/ezv059 Advance Access publication 26 February 2015

ORIGINAL ARTICLE

Cite this article as: Contino M, Mangini A, Lemma MG, Romagnoni C, Zerbi P, Gelpi G *et al*. A geometric approach to aortic root surgical anatomy. Eur J Cardiothorac Surg 2016;49:93–100.

A geometric approach to aortic root surgical anatomy

Monica Contino[a,*], Andrea Mangini[a,b], Massimo Giovanni Lemma[a], Claudia Romagnoni[a], Pietro Zerbi[c], Guido Gelpi[a] and Carlo Antona[a,d]

[a] Cardiovascular Surgery Department, Ospedale Luigi Sacco, Milano, Italy
[b] DEIB Department Politecnico di Milano, Milan, Italy
[c] Pathology Unit, Institute of Biomedical Sciences, Ospedale Luigi Sacco, Milano, Italy
[d] Università degli Studi di Milano, Milan, Italy

* Corresponding author. Cardiovascular Surgery Department, 'Luigi Sacco' University General Hospital, Via G.B. Grassi 74, 20157 Milan, Italy. Tel: +39-02-39042333; fax: +39-02-39042652; e-mail: monica.contino@gmail.com (M. Contino).

Received 25 September 2014; received in revised form 21 January 2015; accepted 23 January 2015

Abstract

OBJECTIVES: The aim of this study was the analysis of the geometrical relationships between the different structures constituting the aortic root, with particular attention to interleaflet triangles, haemodynamic ventriculo-arterial junction and functional aortic annulus in normal subjects.

METHODS: Sixteen formol-fixed human hearts with normal aortic roots were studied. The aortic root was isolated, sectioned at the midpoint of the non-coronary sinus, spread apart and photographed by a high-resolution digital camera. After calibration and picture resizing, the software AutoCAD 2004 was used to identify and measure all the elements of the interleaflets triangles and of the aortic root that were objects of our analysis. Multiple comparisons were performed with one-way analysis of variance for continuous data and with Kruskal–Wallis analysis for non-continuous data. Linear regression and Pearson's product correlation were used to correlate root element dimensions when appropriate. Student's *t*-test was used to compare means for unpaired data. Heron's formula was applied to estimate the functional aortic annular diameters.

RESULTS: The non coronary–left coronary interleaflets triangles were larger, followed by inter-coronary and right-non-coronary ones. The apical angle is <60° and its standard deviation can be considered an asymmetry index. The sinu-tubular junction was shown to be 10% larger than the virtual basal ring (VBR). The mathematical relationship between the haemodynamic ventriculo-arterial junction and the VBR calculated by linear regression and expressed in terms of the diameter was: haemodynamic ventriculo-arterial junction = 2.29 VBR (diameter) + 47.

DISCUSSION: Conservative aortic surgery is based on a better understanding of aortic root anatomy and physiology. The relationships among its elements are of paramount importance during aortic valve repair/sparing procedures and they can be useful also in echocardiographic analysis and in computed tomography reconstruction.

Keywords: Interleaflet triangle • Virtual basal ring • Sinu-tubular junction • Haemodynamic ventriculo-arterial junction • Aortic root • Aortic valve repair

INTRODUCTION

Sparing aortic valve repair procedures and aortic valve repair techniques have changed the surgical view of the aortic root. Features described by anatomists have been integrated by surgeons into their cultural burden, who now look at the aortic valve as a functional unit, as a continuum embracing structure and function. However, there is a part of the aortic root that cardiac surgeons and cardiologists are not familiar with, which is of paramount importance for conservative surgery of the aortic valve and root: the interleaflets triangles.

In this paper, we integrate the anatomical and functional characteristics of the interleaflets triangles with their surgical relevance for aortic valve repair, review the pertinent literature and carefully analyse their topographic anatomy.

MATERIALS AND METHODS

We studied 16 formol-fixed human hearts with normal aortic roots, to specifically review the morphological features of the interleaflets triangle together with their mode of connection to the adjacent structures (Fig. 1); an informed consent was signed by the next-of-kin before proceeding with the heart sectioning. The mean cadaver age was 74 ± 16 years (range: 26–93 years), all of whom were Caucasian; 9 were females. The specimens were prepared for measurements by trimming the ascending aorta 1 cm above the sinu-tubular junction (STJ), and circumferentially dissecting the left ventricular outflow tract 1 cm below the nadir of the Valsalva sinuses. Specimen analysis was made after opening the aortic root longitudinally through the middle portion of the non-coronary Valsalva sinus, in order to keep the interleaflets

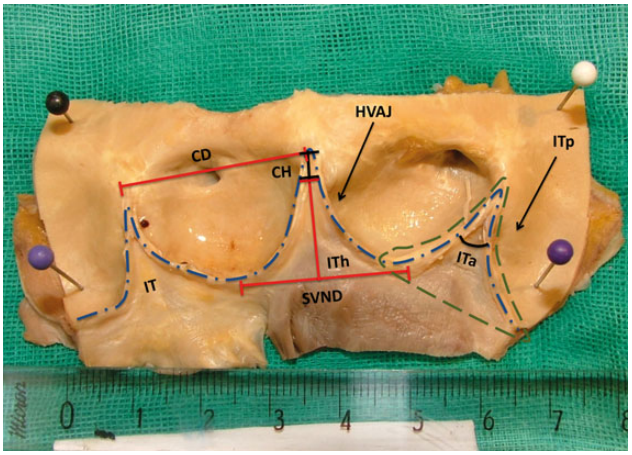

Figure 1: Main elements measured in the aortic root and in the interleaflets triangle. IT: interleaflets triangles; CD: commissural distance; CH: commissural height; ITh: interleaflets triangles height; SVND: sinus of Valsalva nadir distance; HVAJ: haemodynamic ventriculo-aortic junction; ITa: interleaflets triangles angle; ITp: interleaflets triangles perimeter.

triangles intact, and spreading the opened aortic root on a flat surface without stretching it. The specimens were then photographed using a 6.1 mega pixel camera (Nikon D70) at a standard distance of 30 cm, both with the leaflets in place and after their removal. Pictures were then reviewed using a computer-aided design software (AutoCAD®, Auto desk, 2004) for measurement of indirect structures (Fig. 2), an easily reproducible measurement method. A centimetre ruler placed under each specimen and included in the picture allowed software calibration and image sizing with the aid of the command Scale (a scaling factor was determined and then the reference length was set from the drawing and the required new length was specified). The other Autocad tools used for the measurement were Pline (to draw polylines, that is, continuous sequences of straight-line or arc segments that can be closed to form a polygon), Quote (to measure segments length) and Angular quote (to measure the amplitude of angles).

A 10-fold magnification was used to rim the contour of the following elements of the aortic root, which were the object of analysis (Figs 1 and 2).

(i) *Commissural distance*, defined as the straight-line distance between two commissures;

(ii) *haemodynamic ventriculo-arterial junction*, defined as the semilunar hinge-line of the aortic leaflets to the aortic root delimiting the basal attachment of the Valsalva sinuses as described by Anderson [1];

(iii) *sinuses of Valsalva nadir distance*, defined as the straight-line distance between two nadirs of the sinus of Valsalva;

(iv) *interleaflets triangle*, defined as the triangular extension of the ventricular outflow tract bordered laterally and superiorly by the semilunar hinge-lines of two adjacent leaflets that join at the level of the STJ, and inferiorly by the corresponding sinuses of Valsalva nadir distance. We assumed this line as the lower limit of the triangle because, unlike the pulmonary valve whose leaflets are directly attached to the musculature of the right ventricular outflow tract, in the aortic root there is no precise inferior border: the aortic annulus, in fact, has a crown-like shape that strictly follows the leaflets' hinge-lines into the aortic root wall, while inferiorly there is no precise limit between muscular tissue and collagen that appear differently represented along the circumference baseline, and so we used an 'arbitrary' limit [2]. The interleaflets

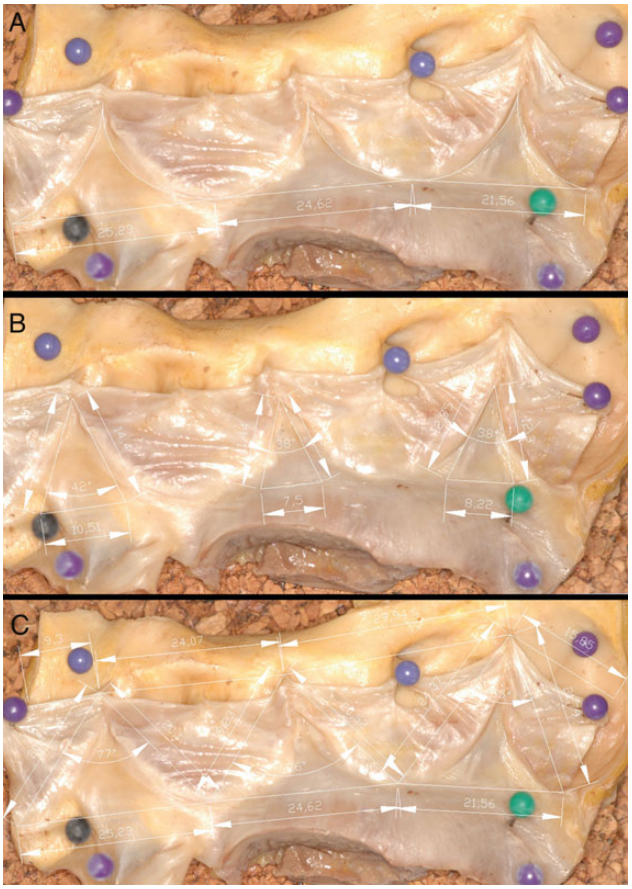

Figure 2: Examples of measurements with the software AutoCAD. (**A**) Extension of the interleaflets triangles and the base length. (**B**) Apex angles' amplitude. (**C**) Measures of the VBR and of sinu-tubular junction by adding the sinuses of Valsalva nadir distances and the commissural distances, respectively.

triangles were further analysed computing the height, perimeter, area and amplitude of the angle below the commissures. (v) *Commissural height*: length of the union between two lines of attachment of the leaflets to the aortic wall at the level of the STJ. To get a first approximation of the STJ, we added the three commissural distances and called this value linear STJ (lSTJ). Similarly, we added the three sinuses of Valsalva nadir distances to obtain the linear virtual basal ring (lVBR). Conscious of the underestimation of these values, we also considered what we named circular STJ (cSTJ) and circular VBR (cVBR). Assuming that the STJ and the VBR are the circumferences passing through the three commissures and the three nadirs, after checking with the Carnot Theorem that the amplitudes of angles were less than 90°, we were able to calculate the cSTJ and the cVBR using Heron's formula, which allows one to obtain the circumcircle of a triangle with known sides (the three commissural distances for the cSTJ and the three nadir distances for the cVBR). Since these values are probably overestimated, to reduce the measurement error, we averaged the linear and the circular data, thus obtaining the estimated STJ and VBR (eSTJ and eVBR).

$$C = 2\frac{abc}{\sqrt{(a+b+c)(a+b-c)(a-b+c)(-a+b+c)}}\pi$$

where a, b and c are the commissural distances (Fig. 3).

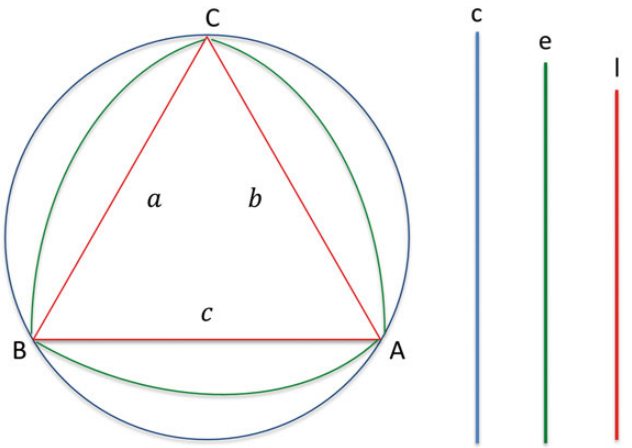

Figure 3: Relationships between circular (c), linear (l) and estimated (e) functional aortic annulus.

$l = a + b + c.$

$$C = 2\frac{abc}{\sqrt{(a+b+c)(a+b-c)(a-b+c)(-a+b+c)}}\pi.$$

$e = (c + l)/2.$

Using the formula of the circumference ($C = 2\pi r$), we calculated the diameters (Table 1). The validation of this method was carried out by a comparison of our results with what is considered the reference value in the literature, if present.

Statistical analysis

The statistical analysis of data was performed using the SPSS® 17.0 software (SPSS, Inc., Chicago, IL, USA) and SigmaPlot© 11.0 (Systat Software, Inc., San Jose, CA, USA). We verified the normality of data with the Shapiro–Wilk test. Continuous data are presented as means ± standard deviations (SDs) and non-continuous data as median (25°–75° percentile). Multiple comparisons were performed with one-way analysis of variance for continuous data and with Kruskal–Wallis analysis for non-continuous data. Linear regression and Pearson's product correlation were used to correlate root elements' dimensions when appropriate. Student's *t*-test was used to compare means for unpaired data. A two-tailed *P*–value of <0.05 was considered statistically significant.

RESULTS

Direct and estimated measurements of the aortic root are reported in Tables 1, 2 and 3. Statistically significant differences were found at the level of interleaflets triangles for the sinuses of Valsalva nadir distance (corresponding to the base of the triangle) ($P = 0.00$), perimeter ($P = 0.00$) and area ($P = 0.01$). There were no statistically significant differences for apical angle ($P = 0.45$), triangle height ($P = 0.53$), commissural distances ($P = 0.09$), commissural height ($P = 0.21$) and haemodynamic ventriculo-arterial junction ($P = 0.10$), whose average length was 103.64 ± 7.23 mm. The eSTJ resulted greater than the eVBR (circumference: 85.38 ± 8.60 vs 77.67 ± 7.41 mm—difference 10%, diameter 27.19 ± 2.74 vs 24.74 ± 2.36 mm—difference 10%) with a eSTJ/eVBR ratio of 1.11 ± 0.17.

The interleaflets triangles component of the VBR were the following: non-coronary–left coronary triangle 36.6 ± 3.14% (25.34 ± 2.9 mm, min 19, max 29.49), left coronary–right coronary triangle 32.34 + 3.3% (22.41 ± 3.16 mm, min 16.94, max 26.8) and

Table 1: Direct and estimated measurements of functional aortic annulus

		Aortic root specimens															Mean
		1	2	3	4	5	6	7	8	9	10	11	12	13	14	15	16	
lSTJ	C	79.16	74.74	59.01	65.93	85.28	75.12	76.50	72.99	80.28	82.79	76.81	85.82	86.41	82.84	67.10	75.86	76.67 ± 7.69
	d	25.21	23.8	18.79	21	27.16	23.92	24.36	23.24	25.57	26.37	24.46	27.33	27.52	26.38	21.37	24.16	24.42 ± 2.45
cSTJ	C	97.38	92.31	72.93	79.69	103.27	92.88	95.95	89.00	97.44	103.02	93.23	106.13	105.73	102.24	82.28	92.10	94.10 ± 9.54
	d	31.01	29.40	23.23	25.38	32.89	29.58	30.56	28.34	31.03	32.81	29.69	33.80	33.67	32.56	26.20	29.33	29.97 ± 3.04
eSTJ	C	88.27	83.53	65.97	72.81	94.27	84.00	86.23	80.99	88.86	92.90	85.02	95.97	96.07	92.54	74.69	83.98	85.38 ± 8.60
	d	28.11	26.60	21.01	23.19	30.02	26.75	27.46	25.79	28.30	29.59	27.08	30.56	30.60	29.47	23.79	26.74	27.19 ± 2.74
lVBR	C	71.41	68.11	61.38	63.34	67.88	79.89	74.18	65.72	68.1	80.06	70.65	59.23	57.48	77.31	73.18	67.03	69.06 ± 6.82
	d	22.74	21.69	19.55	20.17	21.62	25.44	23.62	20.93	21.69	25.5	22.5	18.86	18.31	24.62	23.31	21.35	21.99 ± 2.17
cVBR	C	86.82	93.62	88.02	76.85	84.58	97.76	90.62	85.23	82.69	99.97	86.64	72.41	69.50	95.16	88.47	82.41	86.30 ± 8.46
	d	27.65	29.82	28.03	24.47	26.93	31.13	28.86	27.14	26.33	31.84	27.59	23.06	22.13	30.30	28.17	26.25	27.48 ± 2.69
eVBR	C	79.12	80.86	74.70	70.09	76.23	88.82	82.40	75.48	75.40	90.01	78.65	65.82	63.49	86.23	80.82	74.72	77.68 ± 7.41
	d	25.20	25.75	23.79	22.32	24.28	28.29	26.24	24.04	24.01	28.67	25.05	20.96	20.22	27.46	25.74	23.80	24.74 ± 2.36

STJ: sinu-tubular junction; VBR: virtual basal ring; c: circular. l: linear; e: estimated; C: circumference; d: diameter.

Table 2: Aortic root measurements

		Aortic root specimens																Mean	*P*-value
		1	2	3	4	5	6	7	8	9	10	11	12	13	14	15	16		
	LC	24.07	20.30	15.79	21.96	28.64	26.21	26.35	26.72	26.01	24.51	25.43	26	26.19	31.09	20.64	26.75	24.79 ± 3.64	
CD	RC	29.94	26.44	21.32	22.26	29.58	28.39	30.02	23.59	29.22	32.21	27.32	26.68	28.16	29.00	25.13	25.78	27.19 ± 3.00	0.09
	NC	25.15	28.00	21.90	21.71	27.06	20.52	20.13	22.68	25.05	26.07	24.06	33.15	32.06	22.75	21.33	23.33	24.68 ± 3.84	
	LC	38.56	36.65	33.26	29.61	40.24	36.23	37.33	33.09	33.92	34.55	38.67	31.67	32.55	38.36	33.96	36.71	35.34 ± 2.95	
HVAJ	RC	35.85	32.67	29.06	31.62	36.87	36.37	34.06	30.49	33.03	34.43	34.21	30.36	29.78	36.86	33.05	34.80	33.34 ± 2.54	0.10
	NC	38.04	36.58	34.87	30.68	35.29	36.94	32.90	34.28	33.41	39.09	36.74	30.49	30.69	35.92	37.16	36.24	34.96 ± 2.68	
	NC-LC	2.09	4.52	3.37	6.82	7.25	6.02	7.31	8.72	4.86	6.04	4.58	7.28	7.92	8.82	5.20	7.00	6.11 ± 1.89	
CH	LC-RC	4.67	5.77	6.17	5.58	5.90	9.19	5.47	7.30	4.53	8.19	10.13	5.92	7.12	9.11	11.03	7.20	7.08 ± 1.95	0.21
	RC-NC	8.33	4.80	7.61	6.09	7.61	5.32	10.96	5.96	4.71	5.41	8.45	7.75	9.45	8.72	7.04	6.79	7.19 ± 1.76	
	NC-LC	25.23	29.45	27.12	21.6	25.42	29.49	27.35	24.05	24.30	29.07	25.95	21.68	19.00	25.69	24.83	25.22	25.34 ± 2.90	
SVND	LC-RC	24.62	20.75	16.94	19.56	25.24	26.80	22.67	20.28	21.30	20.33	24.64	20.18	19.60	29.16	24.28	22.17	22.41 ± 3.16	0.00
	RC-NC	21.56	17.91	17.32	22.18	17.22	23.60	24.16	25.39	22.50	30.66	20.06	17.37	18.88	22.46	24.07	19.64	21.56 ± 3.63	
eSTJ	C	88.27	83.53	65.97	72.81	94.27	84.00	86.23	80.99	88.86	92.90	85.02	95.97	96.07	92.54	74.69	83.98	85.38 ± 8.60	
	d	28.11	26.60	21.01	23.19	30.02	26.75	27.46	25.79	28.30	29.59	27.08	30.56	30.60	29.47	23.79	26.74	27.19 ± 2.74	
eVBR	C	79.12	80.86	74.70	70.09	76.23	88.82	82.40	75.48	75.40	90.01	78.65	65.82	63.49	86.23	80.82	74.72	77.68 ± 7.41	
	d	25.20	25.75	23.79	22.32	24.28	28.29	26.24	24.04	24.01	28.67	25.05	20.96	20.22	27.46	25.74	23.80	24.74 ± 2.36	

CD: commissural distance; HVAJ: haemodynamic ventriculo-aortic junction; CH: commissural height; SVND: sinuses of Valsalva nadir distance; ITb: interleaflets triangles base; eSTJ: estimated sinu-tubular junction; eVBR: estimated virtual basal ring; LC: left coronary sinus; RC: right coronary sinus; NC: non-coronary sinus; C: circumference; d: diameter.

Table 3: Measurements of the interleaflets triangles

		Aortic root specimens														Mean/median	*P*-value
		1	2	3	4	5	6	7	8	9	10	11	12	13	14	15	16		
lTang	NC-LC	42	44	46	62	41	61	62	52	57	53	52	48	50	41	44	49	50.25 ± 7.27	0.45
	LC-RC	38	28	28	37	40	50	31	60	46	41	54	50	44	62	72	46	45.44 ± 12.39	
	RC-NC	38	32	28	46	38	48	58	70	50	62	55	48	61	53	55	31	48.31 ± 12.17	
	NC-LC	13.75	10.00	11.78	7.74	11.72	8.76	10.13	12.70	10.22	10.54	13.10	9.45	12.18	11.58	11.69	13.70	11.19 ± 1.74	
lTh	LC-RC	10.91	9.15	8.92	10.13	14.69	9.32	12.57	8.94	11.79	8.88	11.41	9.69	10.96	10.73	7.21	12.10	10.46 ± 1.82	0.41
	RC-NC	11.93	12.19	11.45	10.68	12.29	12.91	6.13	7.65	9.68	8.98	10.25	9.57	8.71	10.99	11.15	12.10	10.42 ± 1.87	
	NC-LC	65.99	70.02	66.19	50.27	64.08	66.30	63.51	60.93	58.60	68.28	67.15	53.48	52.46	93.10	62.90	63.37	62.29 ± 5.80	
lTp	LC-RC	60.99	53.49	44.39	50.10	67.06	62.45	61.16	49.58	54.83	50.22	60.77	51.73	51.25	68.46	54.13	57.44	56.13 ± 6.79	0.00
	RC-NC	56.89	50.51	47.98	54.88	49.14	60.68	53.79	57.06	55.02	69.63	52.34	46.54	46.8	56.89	60.33	53.98	54.53 ± 5.97	
	NC-LC	86.48	68.66	87.17	45.65	74.03	73.16	85.97	98.98	71.96	86.04	76.35	48.13	60.44	80.73	63.51	138.4	75.19 (67.37–86.15)	
lTa	LC-RC	59.92	41.59	35.05	50.30	100.05	62.08	64.32	47.66	78.06	41.18	84.11	41.90	54.35	81.36	49.28	73.50	57.14 (46.22–74.64)	0.01
	RC-NC	61.02	62.99	57.41	69.50	61.61	94.36	35.46	52.39	53.01	62.30	45.62	53.13	44.64	62.53	61.89	55.62	59.22 (52.86–62.36)	

lTang: interleaflets triangle angle; lTh: interleaflets triangle height; lTp: interleaflets triangle perimeter; lTa: interleaflets triangle area; NC: non-coronary sinus; LC: left coronary sinus; RC: right coronary sinus.

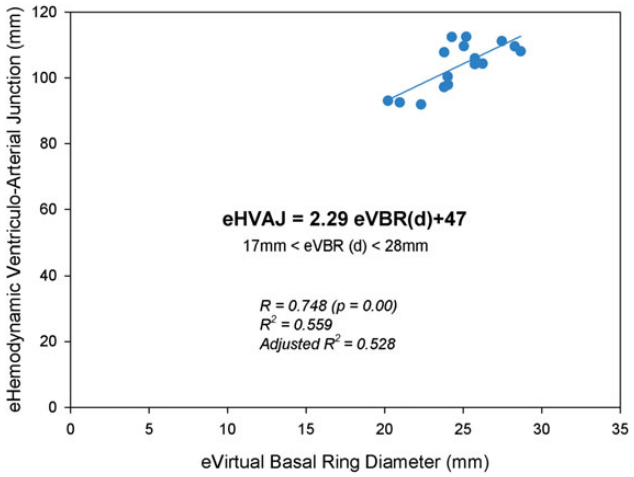

Figure 4: Mathematical relationship between eVBR and eHVAJ calculated by linear regression. eHVAJ: estimated haemodynamic ventriculo-aortic junction; eVBR(d): estimated virtual basal ring diameter.

non-coronary–right coronary triangle 31.05 ± 3.59% (21.56 ± 3.63 mm, min 17.22, max 30.66).

We considered the SD of the apical angle of the interleaflets triangles in every root as an asymmetry index with mean = 8.61 ± 5.93° (min 1.15 in the symmetric root to max 24.78 in the asymmetric root).

The haemodynamic ventriculo-arterial junction was calculated by summing the polylines lengths matching the insertions of the three leaflets. The median eVBR was 77.68 ± 7.41 mm with a calculated diameter of 24.74 ± 2.36 mm and the haemodynamic ventriculo-arterial junction was 103.64 ± 7.23 mm (the ratio between the haemodynamic junction and the eVBR 1.34 ± 0.08). The mathematical relationship calculated by linear regression and expressed in terms of diameter was: estimated haemodynamic ventriculo-arterial junction = 2.29 eVBR(d) + 47 with a VBR d range from 17 to 28 mm ($\lim_{d\to\infty}$ haemodynamic ventrico-arterial junction = VBR) (Fig. 4). The Pearson product moment correlation showed an $R = 0.75$ ($P = 0.00$), $R^2 = 0.56$ with an adjusted $R^2 = 0.53$ and a standard error of estimate = 4.96.

DISCUSSION

Conservative aortic valve surgery is based on a better understanding of aortic root anatomy and dynamics. The aim of this work was the achievement of anatomical information about this functional unit, in order to improve surgical reparative techniques already in use. During data collection, particular attention was given to interleaflets triangles since they are positioned between the anatomical and the functional ventriculo-arterial junction, and to the geometric relationships between the different elements belonging to the aortic root. The aortic root changes its overall configuration from a cone to a cylinder, and from a cylinder to an inverted cone, following ventricular filling and contraction. The interleaflets triangles is the space delineated by two consecutive sinuses of Valsalva, their function is very important for the physiological functioning of the annulus. Systolic expansion of the aortic root is estimated to increase the aortic root inlet (the so-called VBR) by between 5 and 15%; this expansion is accomplished through the interleaflets triangles in an asymmetric way in order to minimize the pressure drop between the left ventricle and the

aortic root. Moreover, interleaflets triangles have an important contribution in absorbing the diastolic load, particularly in end-diastole [3].

As previously mentioned, interleaflets triangles are the areas surrounded by the semilunar attachments of the valvar leaflets beneath the commissures (Fig. 1). Their histology has been already described by Sutton *et al*. [4]: the tissue is composed of a thin, primarily circularly oriented layer of collagen fibres and light staining acellular material; their surface corresponds to the 54% of the total circumference at the level of the nadir of the Valsalva sinuses. Their anatomical relationship are well defined in two papers by Anderson [1] and Ho *et al*. [5]; their kinematics is explained by the works of Dagum *et al*. [6] and Lansac *et al*. [7] in sheep models. Grousson *et al*. [8] described, using a complex 3D digitizer, in a very elegant paper in the Journal of Biomechanics, the modification of the leaflets' attachment lines during the cardiac cycle, taking into account the intersections of different planes; unfortunately the paper lacks simple and usable information in clinical practice. Interleaflets triangles' dimensions and their geometrical characteristics in human beings have not been completely described to the best of our knowledge. In 1975, McAlpine [9] had already pointed to these areas as potential sites of aneurysmal formation because interleaflets triangles are thinner and less collagenous than the hinge-lines of the sinuses of Valsalva wall. Nevertheless, recent studies discovered that cells of the interleaflets triangles may express a range of cytoskeletal and contractile proteins as vimentin, desmin and smooth muscle a-actin, indicating that these structures may be involved in the regulation of aortic root function [10].

The use of the term 'anulus' and its meanings should be carefully considered, since this word is used in different ways by the different experts. Echocardiographers measure the circumference defined by the nadirs of the semilunar leaflets insertion line into the aortic wall as the aortic valve annulus; that is what we call the VBR. From a strictly anatomical point of view, we speak about the annulus pointing out the limit between left ventricular muscular tissue and the collagen tissue, which corresponds to the anatomical ventriculo-arterial junction. From a surgical point of view, the haemodynamic ventriculo-arterial junction is defined as the semilunar hinge-line of the aortic leaflets to the aortic root delimiting the basal attachment of the sinuses of Valsalva, which consists of dense fibrous tissue, partially used for surgical fixation of some prosthetic valves. In particular, looking at the relationships between the anatomical and haemodynamic ventriculo-arterial junction, we observe that the hinge-line of the right and left coronary leaflets cross the anatomical venticulo-arterial junction. Even though Sievers *et al*. [11], in a very interesting review about aortic valve and root terminology, suggest to use the term annulus to define the VBR, as commonly accepted, we do not agree with this classification and terminology and we prefer to follow the one proposed by Anderson, which is more correct and complete from an anatomical and physiological point of view.

From our clinical practice we supposed that normal interleaflets triangles are isosceles, while equilateral ones are the result of mild ventriculo-arterial junction dilatation and obtuse-angled ones of severe dilatation, but we did not have precise data. In our analysis, the mean physiological interleaflets triangles apex angle turned out to be 48.46 ± 11.69° (range: 28–72°); thus, we consider 60° (median + 1SD—equilateral triangle) as the cut-off for interleaflets triangles dilatation. This value allows a simple and immediate visual examination during surgical procedures. On the same basis we considered mild dilatation to be an apex angle between 60 and 90° (from median + 1SD to median + 3SD; from equilateral to right triangle) and that between 90 and 120° (from median + 3SD to median + 6SD; from right to obtuse triangle) to be severe. This dilatation could be symmetric, involving the three triangles in same measure, or asymmetric involving one or two triangles. The apex angle SD could be considered a good symmetry index.

This classification into three different dilatation categories based on the surgical experience of our centre, serves as guidelines of sorts in the choice of the appropriate surgical technique [12]:

(i) In case of aortic regurgitation in the presence of *normal interleaflets triangles* (apical angle amplitude <60°), a subcommissural reshaping should be enough to obtain a better coaptation length and height; if the Valsalva sinuses are dilated, a sparing procedure should be preferred (in this circumstance, also a remodelling can be performed, being the circumference of the VBR of normal dimensions).

(ii) In case of *mild interleaflets triangle dilatation* (apical angle extent between 60 and 90°), the choice of the kind of surgery deeply depends upon the age of the patient: for young people the reimplantation technique is the better solution, while in older patients a less aggressive treatment with a complex aortic valve repair procedure should be considered since, avoiding coronary ostial reimplantation, it would guarantee a quicker cross-clamping time, which is a fundamental aspect to be considered for frail patients.

(iii) In case of severe *interleaflets triangle dilatation* (apical angle amplitude between 90 and 120°), we have two main options: reimplantation technique, or aortic valvuloplasty with addition of an external ring at the level of the VBR. According to our surgical experience, in case of reimplantation procedures some particular tricks could be applied, especially in positioning pledgeted stitches at the level of the proximal suture line. In fact, this technique normally provides the placement of the proximal suture line at the level of the horizontal plane formed by the base of the interleaflets triangles, slightly higher in correspondence with the commissure near the right sinus, because at this point the dissection is limited by the muscle [13]. In case of VBR dilatation, instead of placing all the stitches on the plane identified by the nadirs of the three Valsalva sinuses, at the level of the ITs we position two pledgeted stitches for each triangle, placing them close and parallel to the leaflet insertion line, where the two sides of the triangle start to diverge. The triangle sutures are then passed through the graft in a different plane: each pledgeted stitch is reported on the prosthesis at the corresponding distance from the STJ plane at which they have been positioned in the native triangles. In this case, the distances between the sutures do not have to be respected in order to obtain a subcommissural triangle reshaping, and the two stitches placed on the two sides of the same native triangle must be positioned closer and vertically on the graft. So, when we tie the sutures, the sides of the dilated interleaflets triangle approach one another, increasing the coaptation height and length (Fig. 5) [14]. Thus, we simultaneously stabilize the VBR and improve the functional reserve.

With regard to the dimensions of the interleaflets triangles, their perimeter and area measurements show the same trend: the non-coronary–left coronary triangle is the biggest, followed by left coronary–right coronary triangle and, finally, the non-coronary–right

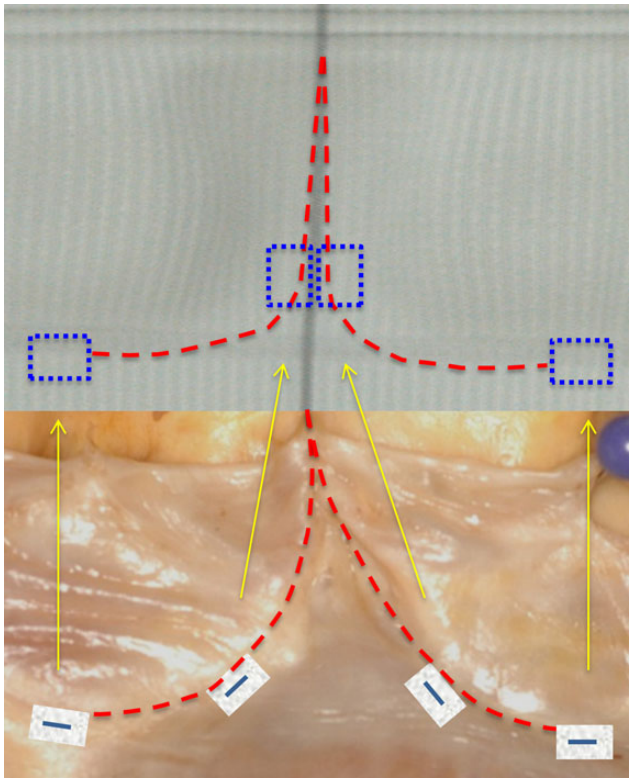

Figure 5: Schematic diagram of the effect of the described technique with the different positioning of the pledgeted stitches on the aortic interleaflets triangles and on the prosthesis. The interleaflets before (below) and after (above) the tying of the stitches are depicted in red.

coronary triangle. Accordingly, the VBR portions corresponding to the three different interleaflets triangles were 36.61 ± 3.14% for the non-coronary–left coronary triangle, 3234 ± 33% for the left coronary–right coronary triangle and 31.05 ± 3.59% for the non-coronary–right coronary triangle.

To better define the inlet and the outflow tract of the aortic root, we decided to average a directly measured but underestimated value with a derived but overestimated one. The direct and underestimated measurements were obtained by summing the three commissural distances for the ISTJ and the three nadir distances for the IVBR; the calculation of the corresponding circular values (derived and overestimated measures) was obtained through Heron's formula; finally, the average between these two values gave us a more precise length of the VBR (eVBR) and of the STJ (eSTJ). We therefore obtained a STJ that is greater than the VBR (eSTJ/eVBR = 1.11 ± 0.17); the ratio between the haemodynamic ventriculo-arterial junction and the VBR was 1.34 ± 0.08. By means of linear regression we also highlighted that the haemodynamic ventriculo-arterial junction is related to the VBR as follows: estimated haemodynamic ventriculo-arterial junction = 2.29 eVBR(d) + 47.

To validate our measurement methodology, we considered the results published in previous papers by other groups. Tops *et al.* [15] found, by a multislice computed tomography on 167 patients, a VBRd in the diastolic phase, closer to our post-mortem analysis, of 24.9 + 2.75 mm (average between coronal and sagittal diameters, considered the VBR elliptical). We compared that result to our eVBRd (24.74 + 2.36; $P = 0.47$ ns), IVBRd (21.99 + 2.17; $P < 0.01$) and cVBRd (27.43 + 2.70; $P < 0.01$), confirming the correctness of our estimating method. Other works [16– 19] seem to confirm these results. Moreover, in a very interesting bioengineering paper, Haj-Ali *et al.* [20] developed a three-dimensional (3D) parametric geometry of the native aortic root merging literature analysis data and a complex root calibrated model based on selective 3D transoesophageal echocardiographic measurements during mid-diastole (298 points); this model seems to perfectly fit and describe our data. In our centre, we also conducted a study (yet to be published), in which we analysed the CT scans of 13 patients with normal aortic root, in which the measurements carried out showed results compatible with the ones obtained here. In these roots we conducted measurements at the level of the VBR that were substantially elliptical, and we found out that the diameter of the IVBR was perfectly comparable with the short-axis diameter of the VBR at this level; the cVBR diameter turned out to be compatible with the long-axis diameter of the VBR at this level; finally, also the eVBR diameter was not statistically significantly different from the mean of the two diameters on the CT scan measurements: this represents an additional demonstration of the feasibility of our method.

All the geometric relationships analysed can be of clinical utility in different fields. First of all, they could be useful to the surgeon both during an aortic valve repair and aortic valve-sparing procedure, to better customize the reshaping technique [14] or to shape the prosthesis in order to obtain an adequate coaptation height and length. Secondly, these geometric connections can be utilized by the cardiologist to estimate, from parameters measurable with the methodology normally adopted, other anatomical structures not directly measurable or detectable (for example, the estimation of the haemodynamic ventriculo-arterial junction from the VBR measurement during standard echocardiographic analysis); all these considerations are of great importance both for research reasons, in the choice of the correct prosthesis and in the selection of the most adequate aortic valve repair techniques. Thirdly, the radiologist could be facilitated in defining by 3D-CT reconstruction the root dilatation at both the levels of the sinuses and the interleaflets triangles. Finally, our estimation methodology allows the execution of aortic root measurements during post-mortem examination; this could be useful to the pathologist to estimate the values under pressure. Furthermore, this could be of great importance in the future for development of a device usable in cardiac surgery for haemodynamic ventriculo-arterial junction stabilization or in optimization of stentless aortic valve design. The eSTJd/eVBRd ratio could be useful to predict the prosthesis diameter to be used in case of ascending aortic replacement with normal VBR and dilatation of the STJ and ascending aorta as already described by Morishita *et al.* [21] using a similar but different geometric approach.

The next step will be the matching of our anatomical data with the CT scan acquired in order to compare them in two different situations, in condition of discharge in aortic root specimens and in physiological configuration under aortic pressure in radiological investigation. 3D-CT scan reconstruction permits to measure similar anatomical findings using comparable tools.

LIMITATIONS OF THE STUDY

This study has some limitations:

(i) The parts of the aortic root as the object of analysis were indirectly measured from pictures of the anatomical specimens using a computer-aided design software (AutoCAD®, Auto

desk, 2004). This approach allows very precise measurements owing to the magnification tool. However, only two of the three dimensions of the space (height and width) could be investigated, it was not possible to compute the depth of the image. In any case, the ratio between different elements of the aortic root functional unit and the interleaflets triangles vertex angle are not influenced by this method of analysis and the error in the third dimension in the diameter measurement seems to be reduced by the procedure we developed to calculate the eVBR and the eSTJ.

(ii) The mean cadaver age was 74 ± 16 years. It is well known that age and body surface area (or more precisely the height, being the body surface area affected by the way of life) affect the shape and dimension of the aortic root and of the ascending aorta [22]. In our series only one heart was from a cadaver younger than 30 years old. Nevertheless, all the ARs were taken from hearts considered normal on 2D echocardiogram during the same hospitalization period.

(iii) Kunzelman *et al.* [23] and Morishita *et al.* [21] reported in formol-fixed specimens that the aortic root was narrower at the VBR level and wider at the STJ level. Our data are in contrast to those in the literature nowadays. We could postulate that our estimating methods could estimate the 'under pressure' root diameter but a larger number of specimens are needed to confirm this hypothesis.

(iv) We used formol-fixed aortic root specimens. Formol allows maintenance of tissue but causes loss of elasticity. We decided to use formol-fixed specimens to guarantee the analysis of all the available hearts at the Departments of Pathology. Ideally, an anatomical study of this functional unit should be carried out using casts of fresh human hearts, being the aortic root cylindrical in shape.

Conflict of interest: none declared.

REFERENCES

[1] Anderson RH. Clinical anatomy of the aortic root. Heart 2000;84:670–3.
[2] Yacoub M, El-Hamamsy I. The Ross operation in infants and children, when and how? Heart 2014;100:1905–6.
[3] Cheng A, Dagum P, Miller DC. Aortic root dynamics and surgery: from craft to science. Philos Trans R Soc Lond B Biol Sci 2007;362:1407–19.
[4] Sutton JP, Ho SY, Anderson RH. The forgotten interleaflet triangles: a review of the surgical anatomy of the aortic valve. Ann Thorac Surg 1995; 59:419–27.
[5] Ho SY, Muriago M, Cook AC, Thiene G, Anderson RH. Surgical anatomy of aorto-left ventricular tunnel. Ann Thorac Surg 1998;65:509–14.
[6] Dagum P, Green RG, Nistal FJ, Daughters GT, Timek TA, Foppiano LE *et al.* Deformation dynamics of the aortic root—modes and physiologic determinants. Circulation 1999;100(Suppl II):II-54–62.
[7] Lansac E, Lim HS, Shomura Y, Lim KH, Rice NT, Goetz W *et al.* A four dimensional study of the aortic root dynamics. Eur J Cardiothorac Surg 2002;22:497–503.
[8] Grousson N, Lim KH, Lim HS, Ooi ET, Salques SL, Yeo JH *et al.* Ventriculo-aortic junction in a human root. A Geometric Approach. J Biomec 2007;40:2167–73.
[9] McAlpine WA. Heart and Coronary Arteries. Berlin, Germany; New York, NY: Springer, 1975.
[10] Dreger SA, Taylor PM, Allen SP, Yacoub MH. Profile and localization of matrix metalloproteinases (MMPs) and their tissue inhibitor (TIMPs) in human heart valves. J Heart Valv Dis 2002;11:875–80.
[11] Sievers HH, Hemmer W, Beyersdorf F, Moritz A, Moosdorf R, Lichtenberg A *et al.* The everyday used nomenclature of the aortic root components: the tower of Babel? Eur J Cardiothorac Surg 2012;41:478–82.
[12] Mangini A, Contino M, Romagnoni C, Lemma M, Gelpi G, Vanelli P *et al.* Aortic valve repair: a ten-year single-centre experience. Interact CardioVasc Thorac Surg 2014;19:28–35.
[13] Boodhwani M, De Kerchove L, El Khoury G. Aortic root replacement using the reimplantation technique: tips and tricks. Interact CardioVasc Thorac Surg 2009;8:584–6.
[14] Mangini A, Lemma MG, Soncini M, Votta E, Contino M, Vismara R *et al.* The aortic interleaflet triangles annuloplasty: a multidisciplinary appraisal. Eur J Cardiothorac Surg 2011;40:851–7.
[15] Tops LF, Wood DA, Delgado V, Schuijf JD, Mayo JR, Pasupati S *et al.* Noninvasive evaluation of the aortic root with multislice computed tomography implications for transcatheter aortic valve replacement. JACC Cardiovasc Imaging 2008;1:321–30.
[16] D'Andrea A, Cocchia R, Riegler L, Scarafile G, Salerno G, Gravino R *et al.* Aortic root dimension in elite athletes. Am J Cardiol 2010;105:1629–34.
[17] Delgado V, Ng ACT, Schuijf JD, Van De Veire NRL, De Roos A, Kroft LJM *et al.* Ann Thorac Surg 2011;91:716–23.
[18] De Kerchove L, El Khoury G. Anatomy and pathophysiology of the ventriculo-aortic junction: implication in aortic valve repair surgery. Ann Cardiothorac Surg 2013;2:57–64.
[19] Vriz O, Driussi C, Bettio M, Ferrara F, D'andrea A, Bossone E. Aortic root dimensions and stiffness in healthy subjects. Am J Cardiol 2013;112: 1224–29.
[20] Haj-Ali R, Marom G, Zekry SB, Rosenfeld M, Raanani E. A general three-dimensional parametric geometry of the native aortic valve and root for biomechanical modeling. J Biomech 2012;45:2392–97.
[21] Morishita K, Murakami G, Koshino T, Fukada J, Fujisawa Y, Mawatari T *et al.* Aortic root remodeling operation: how do we tailor a tube graft? Ann Thorac Surg 2002;73:1117–21.
[22] Wolak A, Gransar H, Thomson LE, Friedman JD, Hachamovitch R, Gutstein A *et al.* Aortic size assessment by noncontrast cardiac computed tomography: normal limits by age, gender and body surface area. JACC Cardiovasc Imaging 2008;1:200–9.
[23] Kunzelman KS, Grande KH, David TE, Cochran RP, Terrier ED. Aortic root and valve relationship – Impact on surgical repair. J Thorac Cardiovasc Surg 1994;107:162–70.